ISO 9001 - 2015

ISSN 2349 - 4891

Monthly

IJRRAS

IF 4.665

Volume 4,Issue 3, March 2017

International Journal of Recent Research and Applied Studies

SURRAGH PUBLICATIONS
SURRAGH PUBLICATIONS

Original Article

ISSN: 2349 - 4891

International
Journal of Recent Research and Applied Studies
(Multidisciplinary Open Access Refereed e-Journal)

Fabrication of Gold Nano Drug by Root Aqueous extract of *Anacyclus pyrethrum for* Pharmacological Applications

G. Subasri[1, 2] & S. Ahmed John[2]

[1]*Post graduate and Research Department of Botany, Kunthavai Naacchiyar Govt. Arts College for Women (Autonomous), Thanjavur - 613007, Tamil Nadu, India.*
[2]*Post graduate and Research Department of Botany, Jamal Mohamed College, affiliated to Bharathidasan University, Tiruchirappalli – 620 020, Tamil Nadu, India.*

Received 10th February 2017, Accepted 1st March 2017

Abstract

The effect of nanoparticles on the natural environment is of growing concerns among environmental scientists and the wider community. Both the fate and behaviour of the nanoparticles in the environment and their effects on the living organisms need to be better understood in order to maintain environmental health and ensure the sustainability of the important nanotechnology industry. Gold nanoparticles are usually synthesized by chemicals which are quite toxic and flammable in nature. This study deals with an environment friendly and biosynthesis process for pharmacological applications of gold nanoparticles, derived from Anacyclus pyrethrum root aqueous extract. The formation and characterisation of AuNPs were confirmed by UV-Vis spectroscopy, Fourier transform infrared spectroscopy (FTIR), scanning electron microscope *(SEM) with energy-dispersive spectroscopy (EDX),* Dynamic Light Scattering analyses (Particle size and Zeta potential) *and X-ray diffraction (XRD). The antimicrobial and anticancer activities were carried out against some human pathogenic strains and HeLa Cancerous cells with different concentrations respectively. The Au nanoparticles inhibited the growth of the microbial pathogens and cancer cells significantly, in a dose and duration dependent manner.*

Keywords: *Anacyclus pyrethrum*, God nanoparticles, Antimicrobial activity, Anticancer activity.

Introduction

Metal nanoparticles have gained a lot of attention due to their unique chemical, optical, magnetic, mechanical, and electric magnetic properties. Nanotechnology is a tremendously powerful technology, which holds a huge promise for the design and development of many types of novel products with its potential medical applications on early disease detection, treatment, and prevention (Sinthiya and Koperuncholan, 2015). Gold nanoparticles represent a new class of biocompatible vectors capable of fulfilling this promise by selective cell and nuclear targeting of which will provide new means for the site- specific diagnosis and treatment of medical conditions. This work outlines the methodology for conjugation of AuNps with target specific biomolecules and details the results of studies assessing the target specificity and Cytotoxicity effects of thus conjugated gold nanoparticles.

Gold Nanoparticles are traditionally synthesized by reducing metallic gold in +3 state to nanoparticulate gold in +1 state. There are a number of reducing agents reported in the literature for the synthesis of AuNps.

Naturally occurring, FDA approved non-toxic compounds such as starch; gum arabic and gelatin were used to stabilize AuNps immediately after they are formed. Gold nanoparticles; due to their ease of synthesis, uniform size distribution, rich surface chemistry and a lack of toxicity; have been proven to be excellent candidates for conjugation with numerous biomolecules for site-specific delivery (Koperuncholan, 2015). Selective cell and receptor targeting of AuNps are likely to provide new pathways for the targeted delivery of diagnostic/ therapeutic agents (Yang et al. 2005, Chithrani and Chan, 2005). Tkachenko *et al.* showed specific nuclear targeting of AuNps by conjugating them with bovine serum albumin (BSA) using differential contrast microscopy (Hong et al. 2003 and Tkachenko et al. 2006). Gold nanoparticles are used as targeted contrast agents in detecting cervical cancer by tagging them with monoclonal antibodies and oncoproteins associated with human papilomavirus (Tkachenko et al. 2004 and Ramesh et al, 2014). Mercaptoalkyl-oligonucleotide conjugated AuNps have been used in the detection of polynucleotides by plasmon band interactions with the surrounding environment (Sokolov et al. 2003). In particular, Gold nanoshells, when coated with breast tumor marker Her-2, effectively localized in

Correspondence
S.Ahmed John
E-mail: drahmedjohn@gmail.com, Ph. +9194868 72786

the microscopic tumors present in the breast tissue (Elghanian et al. 1997). Most of the work in the area of nanoimaging is also focusing on fabricating detectors that can detect efficiently cells undergoing apoptosis, an effect common to many chemotherapeutic regimens (Koperuncholan and Manogaran, 2015). These examples of the use of AuNPs in medical diagnosis although demonstrate the potential of AuNPs even in drug delivery, their target specificity by conjugation with biomolecules has yet to attain the desired refinement.

Materials and Methods

Sample collection

The *Anacyclus pyrethrum* plant was collected from Thanjavur district, Tamil Nadu, India during November to December 2016.

Aqueous Extraction

The plant materials were collected individually, washed thoroughly thrice with distilled water, shade-dried up to 5 days and prepared fine powder by grinding. The fine powder of the plant material was sterilized at 121°C for 15 min and weighed. Sterilized fine powder, 20 g was taken, mixed with 200 ml of Milli Q water and kept in boiling water bath at 100°C for 10 min. The extracts were filtered with Whatman 1 filter paper and the filtered extracts were stored in a refrigerator at 4°C for further studies to avoid microbial contamination.

Fabrication of gold nanoparticles

The gold chloride prepared at the concentration of 10^{-3} M with pre-sterilized Milli Q water. A quantity of 10 ml plant extract was mixed with 90 ml of 10^{-3} M gold chloride for the synthesis of gold nanoparticles. Gold chloride has taken in similar quantities without adding plant extracts to main respective controls. The saline bottles were tightly covered with aluminium foil in order to avoid photo reduction of gold ions, incubated at room temperature under dark condition and observations were recorded.

Characterization of nanoparticles

After AuNPs. formation, it was characterized by UV-vis spectroscopy (UV spec), Fourier transform-infra red spectroscopy (FTIR), Scanning electron microscope (SEM), energy dispersive spectroscopy (EDS), dynamic light scattering (DLS - particles analyzer/ 'Z' potential) methods and X-ray diffraction (XRD) (Koperuncholan and Ahmed John, 2011).

UV-VIS spectroscopy

The Au nanoparticles were characterized in a Perkin-Elmer UV-VIS spectrophotometer, Lambda-19 to know the kinetic behaviour of Au nanoparticles. The scanning range of the samples was 200-800 nm at a scan speed of 480 mm/min. Baseline correction of the spectrophotometer was carried out by using a blank reference.

Fourier transform-infra red (FT-IR) spectroscopy

The analysis of bio-reducing agent present in each of the extracts was measured by FT-IR. After the reaction, a small aliquot of the concentrated reaction mixture was measured in the transmittance mode at 400 to 4000 cm-1. The spectra of the extracts taken after the biosynthesis of nanoparticles were analyzed.

Scanning electron microscope (SEM) and energy dispersive spectroscopy (EDS)

In this research work, Joel JSM-6480 LV SEM machine was used to characterize the mean particle size and morphology of nanoparticles. Compositional analysis on the sample was carried out by the energy dispersive X-ray spectroscopy (EDS) attached with the SEM. The EDS analysis of Ag sample was done by the SEM (JEOLJSM 5800) machine. The EDS normally reveals the presence of phases.

Dynamic Light Scattering analyses *(Particle size and Zeta potential)*

In order to find out the particle size distribution the Au powder was dispersed in water by horn type ultrasonic processor [Vibronics, model: VPLP1]. Dynamic light scattering (DLS) which is based on the laser diffraction method with multiple scattering techniques was employed to study the average particle size of gold nanoparticles. The prepared sample was dispersed in deionized water followed by ultra-sonication. Then solution was filtered and centrifuged for 15 min. at 25^0C with 5000 rpm and the supernatant was collected. The supernatant was diluted for 4 to 5 times and then the particles distribution in liquid was studied in a computer controlled particle size analyzer (ZETA sizer Nanoseries,Malvern instrument Nano Zs) to find out the particle size distribution.

Zeta potential describes the electrical potential in the double layer of ions surrounding a particle at the boundary of the particle surface and the adsorbed ions in the diffuse layer (Ives, 1956; Henderson, 2008). Zeta potentials were determined with a Zetaphorementer IV (CAD, France).

X-ray diffraction method

The phase evolution of calcined powder as well as that of sintered samples was studied by X-ray diffraction technique (Philips PAN analytical, The Netherlands) using Cu radiation. The generator voltage and current was set at 40 KV and 30 mA respectively. The Au sample was scanned in the range 10.0000 - 90.0000^o in continuous scan mode. The scan rate was 0.60/sec.

Antimicrobial screening AuNPs

The gold nanoparticles were challenged against certain microbial strains (procured from MTCC and NCIM, India) for antimicrobial sensitivity using the disc diffusion method (Bauer and Kirby, 1966; Vignesh et al., 2013; Ahmed John and Koperuncholan, 2012). The test strains were: *Aeromonas liquefactions* MTCC 2645 (B1), *Enterococcus faecalis* MTCC 439 (B2), *Klebsiella pneumonia* NCIM 2883 (B3), *Micrococcus luteus* NCIM 2871 (B4), *Salmonella typhimurium* NCIM 2501 (B5), *Vibrio cholerae* MTCC 3906 (B6), *Candida albicans* MTCC 1637 (F1), *Cryptococcus* sp. MTCC 7076 (F2), *Microsporum canis* MTCC 3270 (F3), *Trichophyton rubrum* MTCC 3272 (F4). A sterile cotton swab was used to inoculate the bacterial and fungal suspension on surface of MHA and PDA agar plates. The 15 and 30 µL of sample coated disc were placed in agar plates, separately. For negative control study, the sterile triple distilled water was used. The plates were incubated at 37±1°C for 24–48 h (for bacteria) and 25 ±1°C for 48-72 h (for fungus). After incubation, the zone of inhibition was measured with ruler. All the trial was performed thrice and mean values were presented.

Determination of Anticancer activity

The AuNPs was dissolved in DMSO, diluted in culture medium and used to treat the chosen cell line (Hela) (obtained from NCCS) over a sample concentration (5 different concentrations – 0.1, 1.0, 10, 25 and 50 µg/mL) range of 0.1 - 50 µg/mL for a period of 24 h and 48 h. The DMSO solution was used as the solvent control. A miniaturized viability assay using 3-(4,5-di-methylthiazol-2-yl)-2,5-diphenyl-2H-tetra-zolium bromide (MTT) was carried out according to the method described by standard procedure (Mosmann, 1983 and Ahmed John and Koperuncholan, 2012a) To each well, 20 µl of 5 mg/mL MTT in phosphate-buffer (PBS) was added and wrapped with aluminum foil, and incubated for 4 h at 37 ^{0}C. The purple formazan product was dissolved by addition of 100 µl of 100 % DMSO to each well. The absorbance was monitored at 570 nm (measurement) and 630 nm (reference) using a 96 well plate reader (Bio-Rad, Hercules, CA, USA). Data were collected for four replicates. Each and used to calculate the respective means. The percentage of inhibition was calculated, from this data, using the formula:

$$\frac{\text{Mean absorbance of untreated cells (control)} - \text{mean absorbance of treated cells (test)} \times 100}{\text{Mean absorbance of untreated cells (control)}}$$

The IC_{50} value was determined as the complex concentration that is required to reduce the absorbance to half that of the control.

Results

Biosynthesis of Au nanoparticles

The plant aqueous solution and gold chloride solutions were prepared separately. The plant extract was mixed with gold chloride for the synthesis of gold nanoparticles. During this process, colour was changed from pale green to pink colour, suggested that formation of gold nanoparticles (Huang et al., 2007 and Fazal Mohamed et al. 2011).

UV-VIS spectral analysis

The UV-VIS spectroscopy studies revealed the presence of beard peaks at 540 nm (Figure 1). The absorption spectra of Au nanoparticles formed in the reaction media have absorbance maxima at 540 nm (Yang et al., 2005 and Koperuncholan and Ahmed John. 2011). A remarkable broadening of peak at around 480 nm to 680 nm indicates that the particles are polydispersed. During each time interval, the peak became distinct and rising. This peak rising clearly denoted the increasing nanoparticles synthesis as the time increases. The intensity of absorption peak increases with increasing time period. This characteristic colour variation is due to the excitation of the SPR in the metal nanoparticles (Vignesh et al. 2012b). The reduction of the metal ions occurs fairly rapidly; more than 90% of reduction of Au+ ions is complete within 2 Hrs. after addition of the metal ions to the plant extract. The metal particles were observed to be stable in solution even 4 weeks after their synthesis. By stability, we mean that there was no observable variation in the optical properties of the nanoparticles solutions with time. On the behalf of UV-vis data it was cleared that reduces metal ions (Vignesh et al. 2014).

Fourier transform infra-red (FTIR) spectroscopy

The synthesized gold nanoparticles were subjected to FT-IR analysis to find out the bioactive compounds synthesized by the plant and associated with the nanoparticles. The FTIR images of the Plant samples show a number of functional bonds associated with them which provide them with stability by capping them. From figure 2, 663 cm-1, 1634 cm-1, 2059 cm-1, 2400 cm-1, 3430 cm-1. The 663 cm-1 corresponds to the C-OH out-of-plane bending, 1634 corresponds to the C=O bond, 2059 cm-1 and 2124 cm-1 corresponds to the C-N bond, 3430 corresponds to the N-H bond. Therefore, the synthesized nanoparticles were surrounded by proteins and metabolites having functional groups. From the analysis of FTIR studies we confirmed that the carbonyl groups from the amino acid residues and proteins has the stronger ability to bind metal indicating that the proteins could possibly from the metal nanoparticles (i.e.; capping of gold nanoparticles) to prevent Agglomeration and thereby stabilize the medium. This suggests that the biological molecules could possibly perform dual functions of formation and stabilization of gold nanoparticles in the aqueous medium. Carbonyl groups proved that flavanones or terpenoids absorbed on the surface of metal nanoparticles. Flavanones or terpenoids could be adsorbed on the surface of metal nanoparticles, possibly by interaction through carbonyl groups or π-electrons in the absence of other strong ligating Agents in sufficient concentration. The presence of reducing sugars in the solution could be responsible for the reduction of metal ions and formation of the corresponding metal nanoparticles (Vignesh et al. 2015a). It is also possible that the terpenoids play a role in reduction of metal ions by oxidation of aldehydic groups in the molecules to carboxylic acids. These issues can be addressed once the various fractions of the plant extract are separated, identified and individually assayed for reduction of the metal ions (Vignesh et al. 2013). This rather elaborate study is currently underway.

Scanning electron microscope (SEM) and energy dispersive spectroscopy (EDS)

The SEM image of gold nanoparticles synthesized by green synthesis process by using 5 % leaves extract and 1mM $HAuCl_4$ concentration it gave a clear image of highly dense gold nanoparticles. The SEM image showing gold nanoparticles synthesized using plant extract confirmed the growth of gold nanostructures (Figure 3).

The EDS reading proved that the compulsory phase of gold (Au) and potassium (K) is present in the sample. It's revealed the presence of pure gold nanoparticles in higher percentages than other factors. This is likely due to the presence of substrate over which the NP sample was held during SEM microscopy (Figure 4). As EDS equipment works at low vacuum (1-270 pa) it allows to observe non-conducting samples without the need to cover them with a thin conductive film, and consequently no evidence of noise by the coating material (Vignesh et al. 2015).

Dynamic Light Scattering of Particle Size analyser

The Figure 5 shows the particle size of the Au nanoparticles samples. After analysing data, it was found that the graphical representation of the average particle size distribution of Au nanoparticles. They were in an orbit of 20-80 nm. However, beyond 100 nm range the percentage of nanoparticles present is high. The highest fraction of Au-NPs present in the solution was 40 nm. From the plot it was apparent that the solution was consist of nanoparticles having various sizes which are indeed in agreement of the result obtained by SEM analysis (Vignesh et al. 2012a and Pandiyarajan et al. 2013).

Dynamic Light Scattering of Zeta Potential Measurement

The Figure 6 shows the zeta potential (ζ) is a measure of the electrostatic potential on the surface of the nanoparticles and is related to the electrophoretic mobility and stability of the suspension of nanoparticles of the nanogold. The overall absorbance of Zeta Potential revealed the energetically very unstable. Therefore, the particles undergo agglomeration/ aggregation to stabilize themselves. So there were some potential charges on the surface of the nanoparticles which makes them stable. These charge potential we got from this analysis. Zeta potential (surface potential) has direct relation with the stability of a form/structure.

XRD analysis

The XRD image of the sample after the addition of the gold chloride hydrate was depicted (Figure 7). Its represents the XRD pattern of the produced gold nanoparticles. The position at 38.1, 44.3, 64.5, 77.7 in peak pattern represents presence of gold and the value is consistent. Although the Figure.7 is in agreement with bragg's reflection values at 2Θ, the produced gold nanoparticles exhibit irregular morphology. The XRD patterns clearly show that the nanoparticles are crystalline in nature.

Antimicrobial studies

The antimicrobial activity assay is the AuNPs were challenged against various NCIM and MTCC microbes using the disc diffusion method. The test concentrations (15 and 30 µL/disc) produce zone on MHA and PDA plates for bacteria and fungi, respectively. The sample was most effective against *Salmonella typhimurium* NCIM 2501 (B5) while smaller effect was noticed from *Micrococcus luteus* NCIM 2871 (B4) in the bacterial division. But in fungi, which was effective against *Trichophyton rubrum* MTCC 3272 (F4) whereas smaller effect was not observed.

The higher (30 µL/disc) concentration got larger zone effect than the small (15 µL/disc) concentration against certain microorganisms. All the microbial strains depict higher sensitivity to the higher concentration (30 µL) for the test sample when compared to the positive control except B3, B4 and B6. There is no antimicrobial activity in solution devoid of sample used as a vehicle control (sterile triple distilled water), reflecting that antimicrobial activity was directly related to the sample (Table 1). The gold nanoparticles not only interact at the surface of cell membrane, but also enter inside the bacteria and cause damage of the cells by interacting with phosphorus/ sulphur containing DNA and its replication (Anitha et al., 2011 and Koperuncholan et al., 2010). In bacteria, the test sample was most effective against B5 while smaller effect was noticed from B4. In fungi, this was effective against F4 whereas smaller effect was observed in F2. All the microbial strains depict higher sensitivity to the higher concentration (30 µL) and he concluded that the silver materials are an efficient alternative to antibiotics for the treatment. This nanoparticles release silver ions in the bacterial cells, which enhance their bactericidal activity (Hussain Beevi et al., 2012 and Vanithamani et al., 2017). There is no antimicrobial activity in solution devoid of sample used as a vehicle control (sterile triple distilled water), reflecting that antimicrobial activity was directly related to the sample.

Anticancer studies

The cytotoxic effect of the AuNPs were examined on Hela cell lines. (Sample conc. = 0.1 – 50 µL). The cytotoxicity effect is very high in biosynthesized AuNPs in all concentrations against Hela cell lines. The AuNPs inhibited the growth of the cancer cells significantly, in a dose and duration dependent manner. The cytotoxic activity was finding according to the dose values of the exposure of the complex required to reduce survival to 50% (IC50), compared to untreated cells. In AuNPs, the 50 µL sample is enough to control cancerous cell. The cytotoxic effect of the sample may be interpretable as due to its amphiphilic nature and, hence, would penetrate the cell membrane easily, reduce the energy status in tumours and also alter hypoxia status in the cancer cell. **(**figure 8)

The cytotoxic effect of the sample may be interpretable as due to its amphiphilic nature and, hence, would penetrate the cell membrane easily, reduce the energy status in tumours and also alter hypoxia status in the cancer cell. The cytotoxicity effect was compared with the standard anticancer drug 5-FU against HeLa cells and their LC_{50} value was observed (Lakshmi praba et al. 2013, Lokina and Narayanan, 2013). Similarly, cytotoxicity of chemically synthesized AuNPs was reported against HeLa cells by Miura and Shinohara. A large number of in vitro studies indicate that AuNPs are toxic to the mammalian cells. Interestingly, some studies have shown that AuNPs has the potential to intervene genes associated with cell cycle progression, also induce DNA damage and apoptosis in cancer cells. Indeed, the results of present study provide conclusive evidence for cytotoxic effect of AgNPs on cancer cell lines rather than normal cell lines.

Acknowledgement

The authors thank the Biospark Biotechnological Research Centre (BBRC), Tiruchirappalli, Tamil Nadu, India for antimicrobial and anticancer studies.

References

1. Ahmed John S and Koperuncholan M, 2012. Antibacterial Activities of various solvent extracts from Impatiens balsamina. International Journal of pharma and bio sciences, 3:401-406.
2. Ahmed John S and Koperuncholan M, 2012a. Direct Root Regeneration and Indirect Organogenesis in *Silybum marianum* and Preliminary Phytochemical, Antibacterial Studies of Its Callus. The International Journal of Pharmaceutics; 2: 52-57.
3. Anitha R, Karthikeyan B, Pandiyarajan T, Vignesh S, Arthur James R, Vishwanathan K, Murari BM. 2011. Antifungal studies on bio-compatible polymer encapsulated silver nanoparticles. Int J Nanosci. 10:1-5.
4. Bauer A W, Kirby W M M, Sherris J C & Turck M, 1966. Antibiotic susceptibility testing by a standardized single disk method. *Amer. I. C/in. Pathol.* 45:493-496.
5. Chithrani BD, Chan WCW, 2007. Elucidating the Mechanism of Cellular Uptake and Removal of Protein-Coated Gold Nanoparticles of Different Sizes and Shapes. *Nano Lett.* 7:1542-1550.
6. Elghanian R, Storhoff JJ, Mucic RC, Letsinger RL, Mirkin CA, 1997. Selective colorimetric detection of polynucleotides based on the distance-dependent optical properties of gold nanoparticles. *Science* 277:1078–1081.
7. Fazal Mohamed M.I, Arunadevi. S, Koperuncholan M and Seeni Mubarak M, 2011. Synthesis and antimicrobial activity of some naphthyl ether derivatives. Pelagia Research Library Der Chemica Sinica; 2: 52-57.
8. Henderson R K Parsons S A and Jefferson B, 2008. Successful removal of algae through the control of zeta potential. Separation Science and Technology. 43:1653-1666
9. Hong R, Han G, Fernandez JM, Kim BJ, Forbes NS, and Rotello VMJ, 2006. Glutathione-Mediated Delivery and Release Using Monolayer Protected Nanoparticle Carriers *J. Am. Chem. Soc.* 128:1078-1079.
10. Huang J Li Q Sun D Lu Y Su Y Yang X Wang H Wang Y Shao W He N Hong J and Chen C, 2007. Biosynthesis of silver and gold nanoparticles by novel sundried Cinnamomum campora leaf. Nanotechnology. 18:104-105.
11. Hussain Beevi M, Vignesh S, Pandiyarajan T, Jegatheesan P, Arthur James R, Giridharan NV and Karthikeyan B. 2012. Synthesis and antifungal studies on CuO nanostructures. Advanced Materials Research. 488-489: 666 - 670.
12. Ives K J 1956. Electrokinetic phenomena of planktonic algae. Proc Soc Water Treat Exam,5:41–53.
13. Koperuncholan M and Ahmed John S. 2011a. Biosynthesis of Silver and Gold Nanoparticles and Antimicrobial Studies of Some Ethno medicinal Plants in South-Eastern Slope of Western Ghats. IJPI'S Journal of Pharmacognosy and Herbal Formulations, 1(5):10-15.
14. Koperuncholan M and Ahmed John S, 2011. Antimicrobial and Phytochemical Screening in Myristica dactyloides Gaertn. Journal of Pharmacy Research, 4: 398-400.
15. Koperuncholan M and Manogaran M, 2015. Edible plant mediated biosynthesis of silver and gold nanoflakes against human pathogens, World Journal of Pharmaceutical Research, 4(1):1757-1775.
16. Koperuncholan M, 2015. Bioreduction of chloroauric acid (HAuCl4) for the synthesis of gold nanoparticles (GNPs): A special empathies of pharmacological activity, International Journal of Phytopharmacy, 5 (4): 72-80.
17. Koperuncholan M, Sathish Kumar P, Sathiyanarayanan G, Vivek G, 2010. Phytochemical Screening and Antimicrobial Studies of Some Ethno medicinal Plants in South-Eastern Slope of Western Ghats. International journal of Medicobiologial Research, 1: 48-59.
18. Lakshmi praba J, Arunachalam S, Riyazuddin R, Divya R, Vignesh S, Akbarsha A and Arthur James R. 2013. DNA/ RNA binding and anticancer/ antimicrobial activities of polymer-copper(II)

complexes. Spectrochimica Acta Part A: Molecular and Biomolecular Spectroscopy. 109:23 – 31.
19. Mosmann T. 1983. Rapid colorimetric assay for cellular growth and survival: application to proliferation and cytotoxicity assays. J Immunological Methods, 65: 55-63.
20. Pandiyarajan T, Udaybhaskar R, Vignesh S, Arthur James R, Karthikeyan B. 2013. Concentration dependent antimicrobial activities of CuO nanoflakes. Material science and engineering C. 33(4): 2020 – 2024.
21. Ramesh V, Ahmed John S and Koperuncholan M, 2014. Impact of cement industries dust on selective green plants: A case study in Ariyalur industrial zone, International Journal of Pharmaceutical, Chemical and Biological Sciences, 4:152-158.
22. Sinthiya A, Koperuncholan M 2015. In-silico characterization for Multiple sclerosis: A special emphasis on Tetrakis (4-aminopyridine-kN1) dichloridocopper (II) monohydrate with sphingosine 1phosphate lyase, Crystal Research. 89: 36824-36826.
23. Sokolov K, Aaron J, Hsu B, Nida D, Gillenwater A, Follen M, MacAulay C, Adler-Storthz K, Korgel B, Descour M, Pasqualini R, Arap W, Lam W, Richards-Kortum R. 2003. Optical systems for in vivo molecular imaging of cancer. *Technol Cancer Res Treat.* 2:491– 504.
24. Tkachenko AG, Xie H, Coleman D, Glomm W, Ryan J, Anderson MF, Franzen S, Feldheim DL. 2003. Multifunctional gold nanoparticle-peptide complexes for nuclear targeting. *J. Am. Chem. Soc.* 125:4700-4701.
25. Tkachenko AG, Xie H, Liu Y, Coleman D, Ryan J, Glomm WR, Shipton MK, Franzen S, Feldheim DL.2004. Cellular trajectories of peptide-modified gold particle complexes: comparison of nuclear localization signals and peptide transduction domains. *Bioconjugate Chem.* 15:482-490.
26. Vanithamani J, Koperuncholan M and Kamaraj M, 2017. A statistical approach of Biochemical Screening with various Biofertilizers and inorganic NPK influence on Amaranthus polygonoids(L.), Statistical Approaches on Multidisciplinary Research, Surragh Publishers, India, 1:104-112.
27. Vignesh G, Arunachalam S, Vignesh S, Arthur James R. 2012a. BSA binding and antimicrobial studies of branched polyethyleneimine - copper (II) bipyridine / phenanthroline complexes. Spectrochimica Acta Part A: Molecular and Biomolecular Spectroscopy. 96: 108 - 116.
28. Vignesh G, Pradeep I, Arunachalam S, Vignesh S, Arthur James R, Arun R and Premkumar K. 2015. Biological and protein-binding studies of newly synthesized polymer–cobalt(III) complexes. Luminescence. DOI 10.1002/bio.2992.
29. Vignesh G, Sugumar K, Arunachalam S, Vignesh S and Arthur James R. 2013. A comparative study on the binding of single and double chain surfactant–cobalt(III) complexes with bovine serum albumin. Spectrochimica Acta Part A: Molecular and Biomolecular Spectroscopy. 113, 415 – 422.
30. Vignesh G, Sugumar K, Arunachalam S, Vignesh S and Arthur James R. 2013. A comparative study on the binding of single and double chain surfactant–cobalt(III) complexes with bovine serum albumin. Spectrochimica Acta Part A: Molecular and Biomolecular Spectroscopy. 113, 415 – 422.
31. Vignesh G, Sugumar K, Arunachalam S, Vignesh S, Arthur James R, Arun R and Premkumar K. 2015. Studies on the synthesis, characterization, human serum albumin binding and biological activity of single chain surfactant–cobalt(III) complexes. Luminescence. DOI 10.1002/bio.2991.
32. Vignesh S, Karthikeyan B, Udayabhaskar R, Arjunan V, Muthukumar K, Ashok M, Narayana Kalkura S, Arthur James R. 2014. Antimicrobial activity of biological green synthesized silver nanoparticles. Asian journal of Physics. 23(6): 1025-1030.
33. Vignesh S, Muthukumar K, James RA. 2012b. Antibiotic resistant pathogens versus human impacts: A study from three eco-regions of the Chennai coast, southern India. Marine Pollution Bulletin. 64:790–800.
34. Yang PH, Sun XS, Chiu JF, Sun HZ, He QY. 2005. Functionalized gold nanoparticles for drug delivery. *Bioconj. Chem.* 16:494-496.

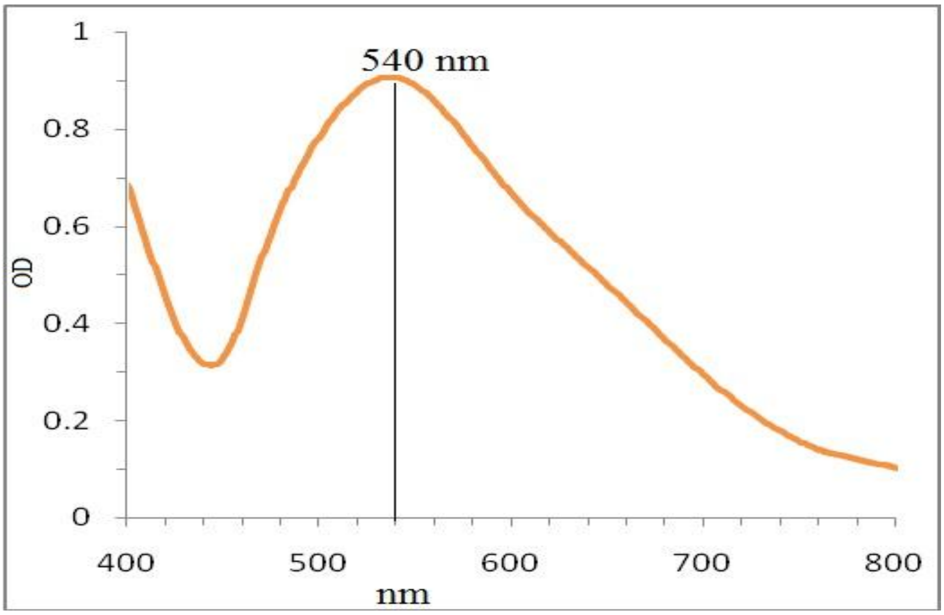

Figure I
UV-Spectrum of AuNPs

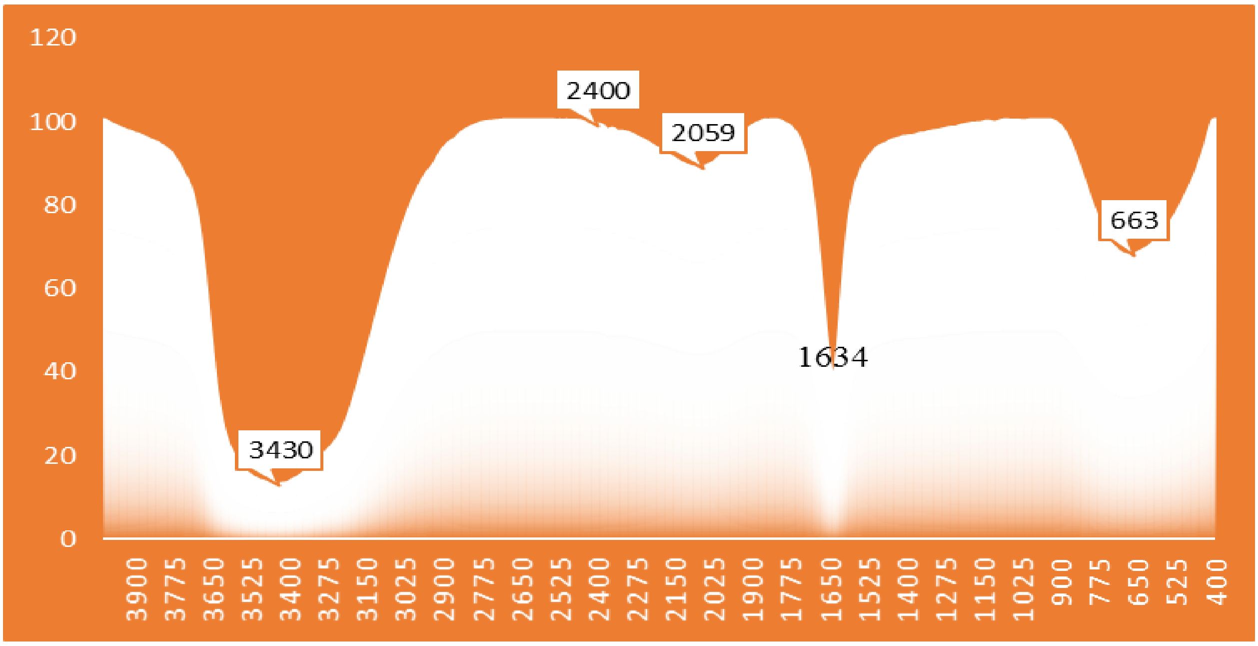

Figure II
FTIR spectrum of AuNPs

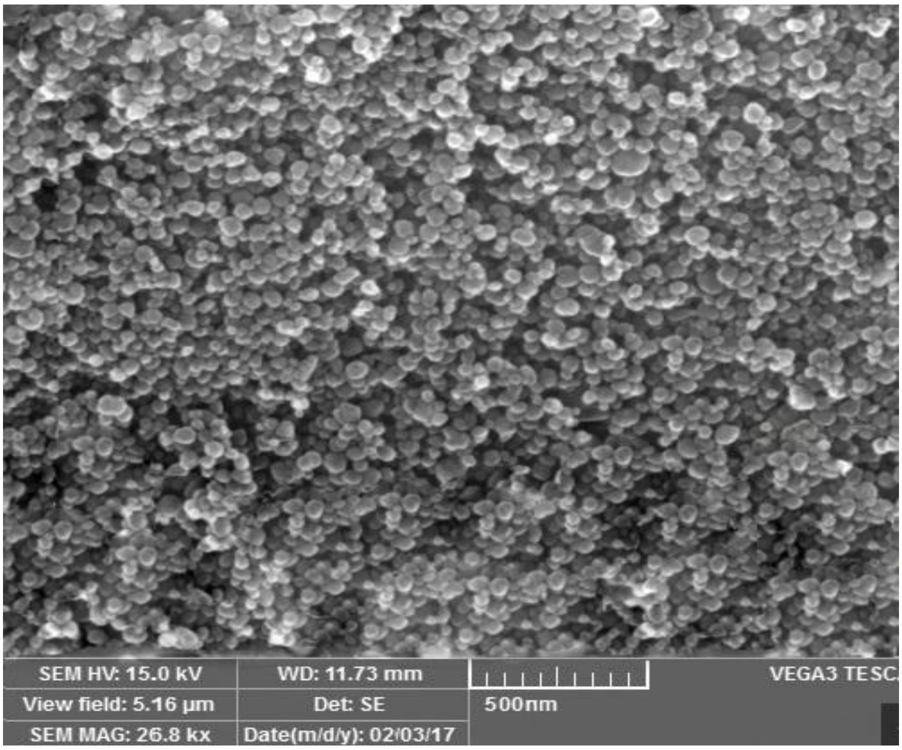

Figure III
SEM Image of AuNPs

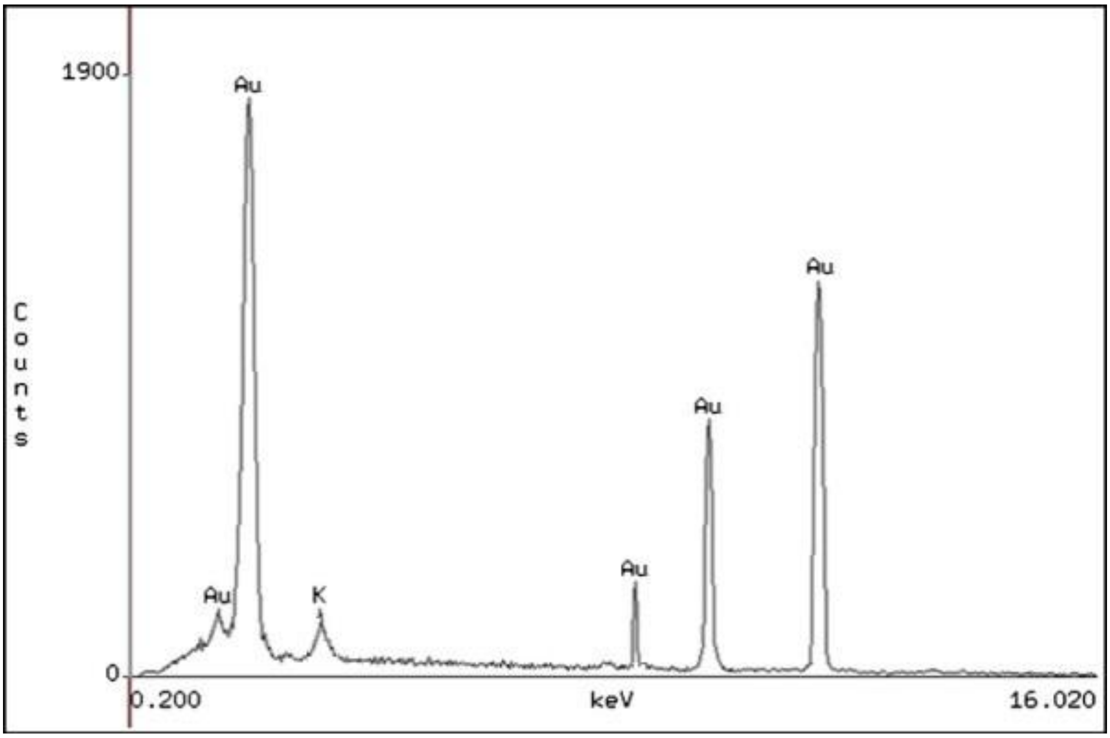

Figure IV
EDAX Spectrum of AuNPs

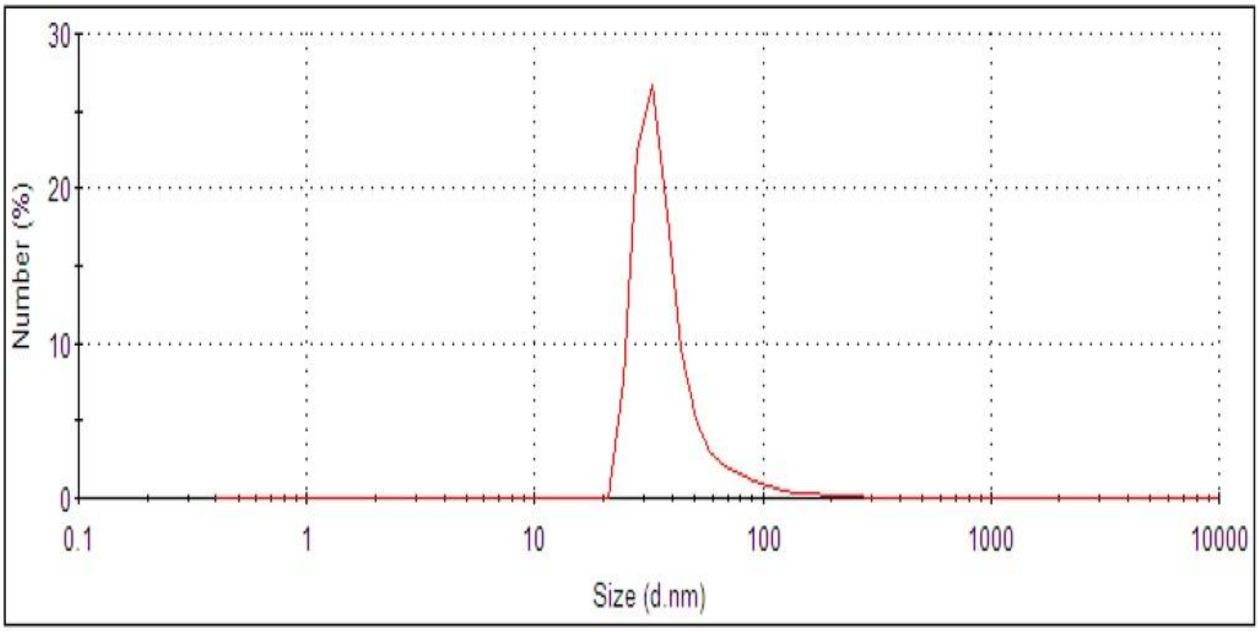

Figure V
DLS-Size distribution of AuNPs

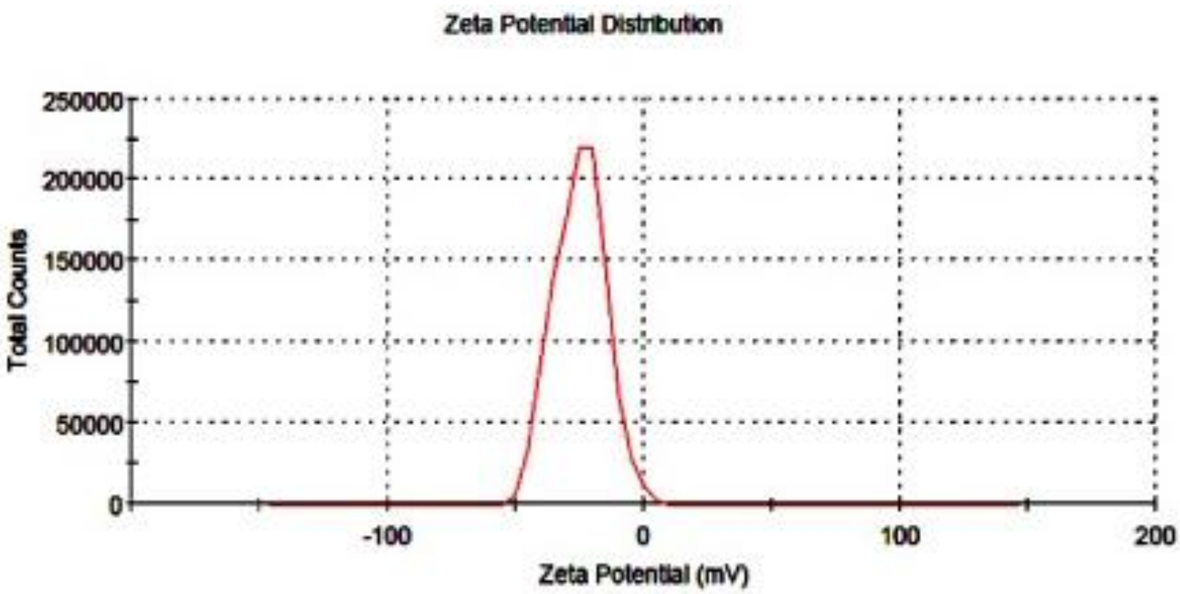

Figure VI
DLS-Zeta Potential of AuNPs

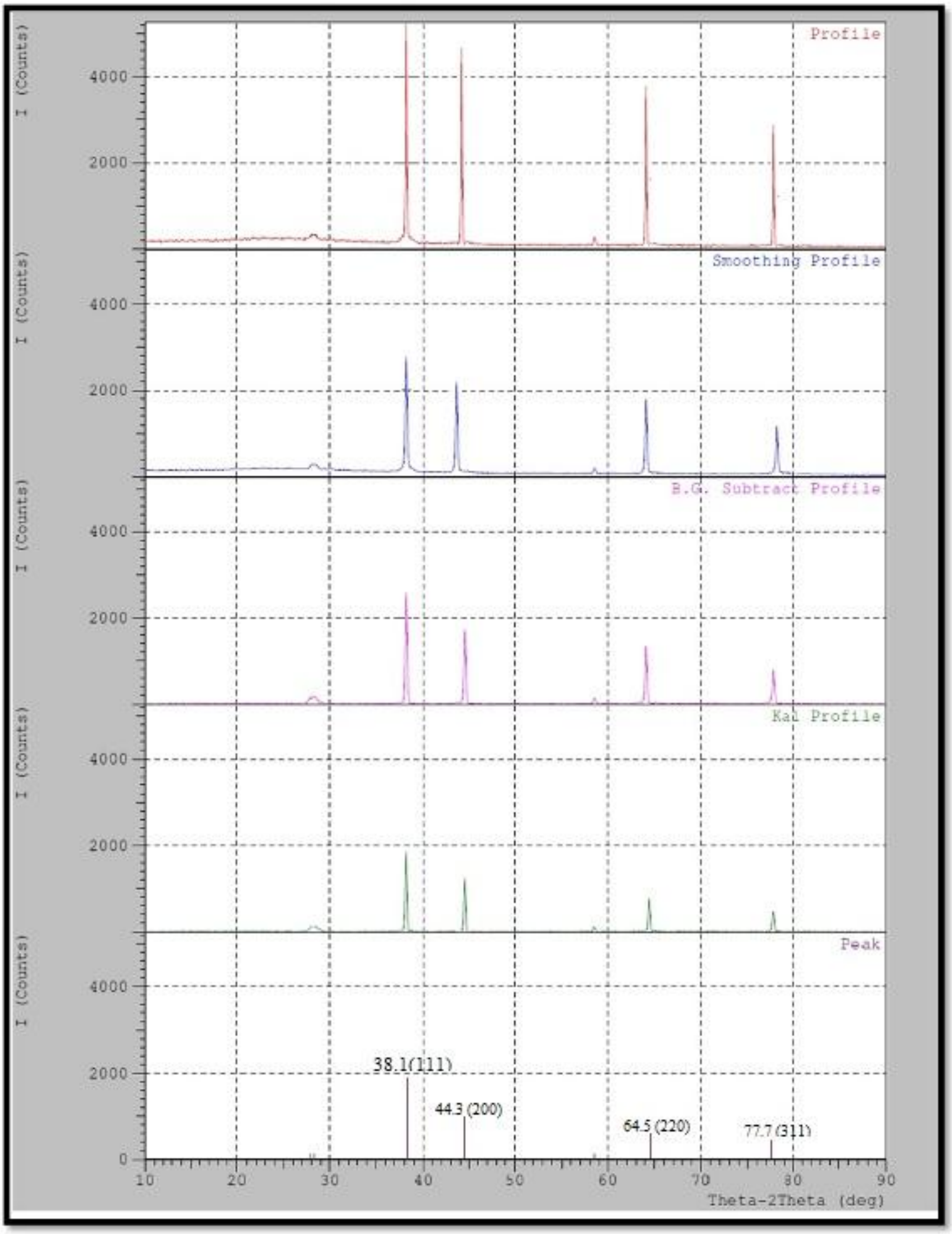

Figure VII
XRD charaterization of AuNPs

Table 1
Antimicrobial activity of AuNPs

S.No	Test Microorganisms	AuNPs µL/disc		PC	Diseases	Route of Transmission
	Bacteria	15	30	10 mcg		
1.	*Aeromonas liquefaciens* B1	12	13	14	Wound Infections / Gastroenteritis	Water / Food
2.	*Enterococcus fecalis* B2	12	14	8	Endocarditis / Epididymal Infections	Water / Food
3.	*Klebsiella pneumoniae* B3	16	18	28	Acute diarrhoea / Dysentery	Water / Food
4.	*Micrococcus luteus* B4	14	19	38	Skin & Pulmonary infections	Soil / Water / Air / Food
5.	*Salmonella typhimurium* B5	12	16	0	Typhoid	Water / Food
6.	*Vibrio cholarae* B6	12	14	16	Cholera	Water / Food
	Fungi					
7.	*Candida albicans* F1	12	14	10	Skin infection / Gastrointestinal tract Infection	Air / Wound / Soil / Water
8.	*Cryptococcus* sp. F2	10	12	9	Bronchiectasis / Endophthalmitis.	Air / Wound / Soil / Water
9.	*Microsporum canis* F3	11	13	9	Tinea capitis /Ringworm	Air / Wound / Soil / Water
10.	*Trichophyton rubrum* F4	13	15	7	Tinea corporis / Tinea pedis	Air / Wound / Soil / Water

PC - Positive Control (Using antibiotic disc; Bacteria – Methicillin (10mcg/disc); Fungi – Itraconazole (10mcg/disc)
Samples – 15, 30 mg/ml (well)

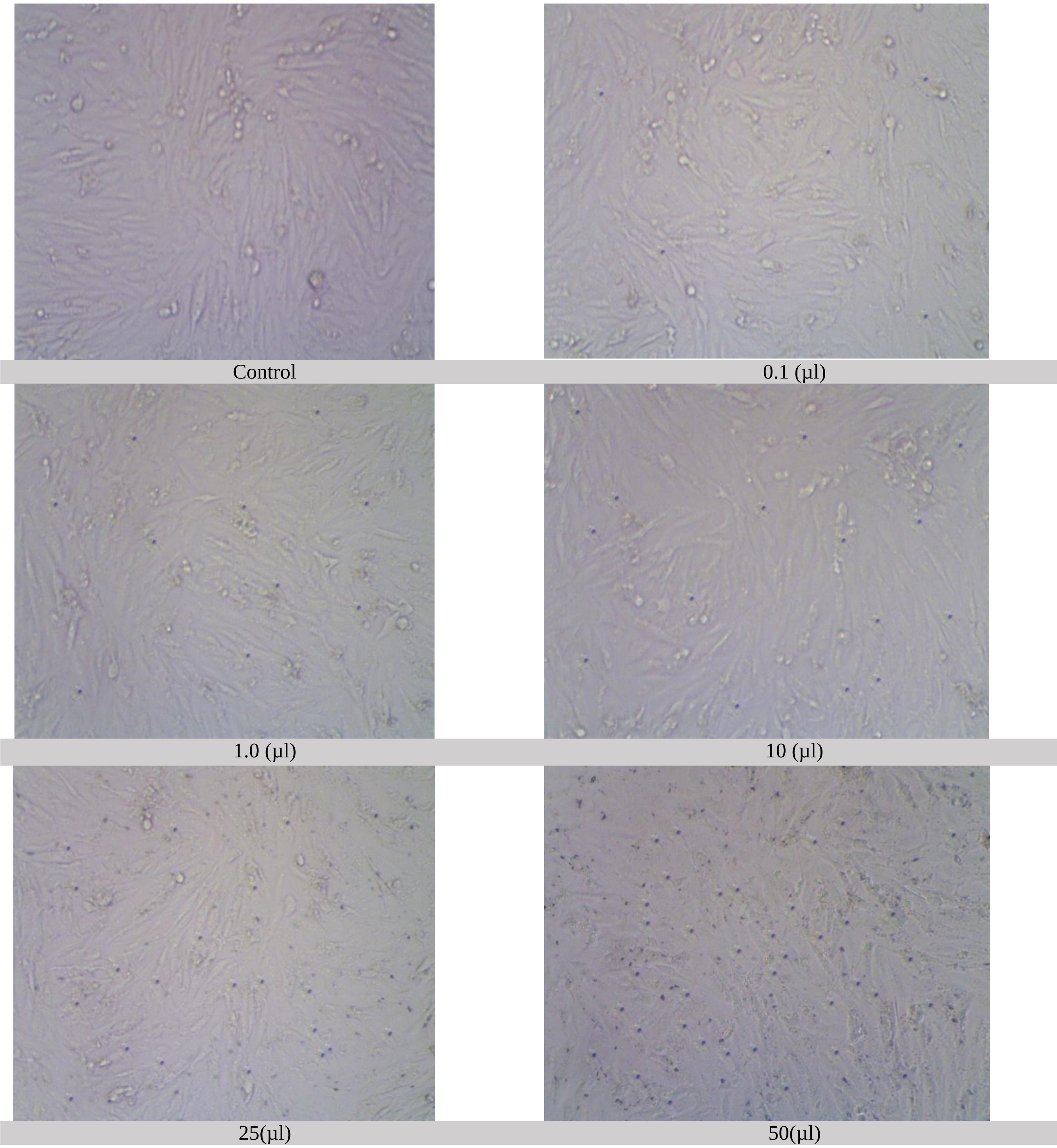

Figure VIII
Anticancer activities of AuNPs